

# The code of the long-term biomass cycles in the Barents Sea

Harald Yndestad

Yndestad, H. 2003. The code of the long-term biomass cycles in the Barents Sea. — ICES Journal of Marine Science, 60: 1251–1264.

Barents Sea capelin (*Mallotus villosus*), Norwegian spring-spawning herring (*Clupea harengus*), and Northeast Arctic cod (*Gadus morhua*) have been associated with large fluctuations of biomass growth. The cause of these large fluctuations has been poorly understood and led to problems in biomass management. The identification of a deterministic cause would provide the possibility of forecasting future biomass fluctuations. In this investigation, the Kola Section sea temperature and the biomasses of capelin, herring, and cod have been analyzed by a wavelet transform to identify the source of the long-term cycles. The wavelet analysis shows that the Kola Section temperature has dominant cycles at the lunar-nodal tide cycles of  $3 \times 18.6 = 55.8$ , 18.5 and  $18.6/3 = 6.2$  years. The recruitment of Barents Sea capelin, Norwegian spring-spawning herring, and Northeast Arctic cod has adopted an optimal recruitment cycle close to the stationary 6.2 years Kola temperature cycle. Long-term biomass growth is correlated to the phase relation between the biomass eigen-frequency cycle and the Kola temperature cycles. The biomasses of capelin, herring and cod have long-term growth when the 6.2 and 18.6 years Kola temperature cycles are positive at the same time. There is a long-term biomass reduction when the temperature cycles are not positive at the same time, and a biomass collapse when the temperature cycles are negative at the same time. The deterministic property of the 18.6 years lunar-nodal tide provides a new way of long-term biomass forecasting over periods of 50–80 years or more.

© 2003 International Council for the Exploration of the Sea. Published by Elsevier Ltd. All rights reserved.

Keywords: biomass eigen-frequency, long-term biomass cycles, wavelet analysis, 18.6-years lunar cycle.

Received 26 June 2002; accepted 28 March 2003.

H. Yndestad: Aalesund University College, Aalesund N-6025, Norway; tel: +47 70 16 12 00; fax: +47 70 16 13 00; e-mail: [harald.yndestad@hials.no](mailto:harald.yndestad@hials.no).

## Introduction

Norwegian records document good herring periods from 1500 to 1570, 1600 to 1650, 1690 to 1774, and from 1808 to 1874 (Vollan, 1971). Since the herring biomass had a fluctuation of about 50–80 years, early marine scientists looked for its fundamental cause. Helland-Hansen and Nansen (1909) analyzed time-series from 1875 to 1905 and found close relationships between variations in the number of sunspots, the quality of cod roe, the quality of cod liver and the anomaly of the mean air temperature at Ona in Norway. These were explained by the periodicity in sunspot occurrence, or rather in the energy received from the Sun, which caused variations in the ocean currents through processes in the atmosphere. They concluded that the sea temperature is only an indicator of the variations from another primary cause.

The Swedish oceanographer Dr. Otto Pettersson [1848–1941] postulated that the orbits of the Moon and the Earth have an influence on long-period tides, climate cycles and

fluctuations of marine biomasses. Pettersson (1905, 1914, 1915, 1930) explained the fluctuation of herring by a tidal 112-year cycle. Later Maksimov and Smirnov (1964, 1965, 1967), Maksimov and Sleptsov-Shevlevich (1970), Loder and Garret (1978), and Royer (1993), identified the 18.6-year lunar-nodal tide in the Atlantic Ocean while Yndestad (1996a, 1999a) found the spectrum of the lunar-nodal tide in the Barents Sea. Ottestad (1942) discovered 11-, 17.5-, 23-, and 57-year cycles in historical records of cod landings in Norway. He compared the estimated cycles with the annual growth-zones of Norwegian pine at Sørfold close to the Lofoten area and concluded that the recruitment of cod is influenced by climate cycles. Hjort (1914) analyzed the length distribution of Northeast Arctic cod. He explained fluctuations in the biomass by a match between the spawning time, on the one hand, and food available to the larvae on the other.

Izhevskii (1961, 1964) reconditioned a system-view of the interacting processes between the hydrosphere, the atmosphere and the biosphere. He argued that the heat in

the ocean is a non-homogeneous system flowing from a warm equator to the cold pole. In this flow of heat, influenced by tidal forces, the ocean influences the atmospheric processes. Izhevskii analyzed the Kola Section temperature data series and estimated cycles of 4–6, 8–10, and 18–20 years. Russian records of the Northeast Arctic cod stock suggested cycles of 8–10 and 18–20 years. In an analysis of Norwegian spring-spawning herring he concluded that cod and herring do not represent substantially different ecological types in terms of their patterns of reproduction. Wyatt *et al.* (1994) analyzed landing records of Northeast Arctic cod from 1885 to 1951 and found a correlation with the 18.6-year nodal tide. Yndestad (1996b, 1999b) reported lunar-nodal cycles of  $18.6/3 = 6.2$ , 18.6, and  $18.6 \times 3 = 55.8$  years in growth and recruitment of Northeast Arctic cod. The same cycles of 6.2 and 18.6 years have been identified in recruitment of the Barents Sea capelin and Norwegian spring-spawning herring (Yndestad and Stene, 2001; Yndestad, 2002).

The Barents Sea capelin, Norwegian spring-spawning herring and Northeast Arctic cod are well described by Gjosæter (1997), Hamre (2000), Toresen and Østvedt (2000), Nakken (1994), and many others. In this paper the long time-series of the sea temperature in the Barents Sea and the separate biomasses of these three species are analyzed to find a common cause for the long-term biomass fluctuations. The investigation is based on a wavelet analysis that identifies the cycle time and phase in dominant biomass fluctuations. The result shows that the long-term fluctuation in the biomass of capelin, herring and cod is caused by a match or mismatch between a biomass eigenfrequency cycle and dominant stationary Kola Section temperature cycles.

## Materials and methods

Russian scientists at the PINRO institute in Murmansk have provided monthly temperature values from the upper 200 m of the Kola Section along the 33°30'E medial from 70°30'N to 72°30'N in the Barents Sea (Bochkov, 1982). The data series from 1900 to 2000 has quarterly values over the period 1906–1920 and monthly values from 1921, partly measured and partly interpolated. In this presentation the annual mean temperature is analyzed.

The time-series of Norwegian spring-spawning herring (*Clupea harengus*) data covers the period 1907–2000. That from 1907 to 1945 are given in Toresen and Østvedt (2000), whilst the information covering 1945–2000 was provided by ICES (2001a).

The time-series for Northeast Arctic cod (*Gadus morhua*) covers the period from 1900 to 2000. That from 1900 to 1945 is based on published estimates from Hysten (2002) and the period from 1946 to 2000 was provided by ICES (2001b). The time-series of Lofoten catch numbers from 1866 to 1957 is given in Godø (2000). From 1958 until

1979 the Lofoten time-series is catch in tons. The data are interpolated to catch numbers by a scaling of 3.5 (tons/1000 numbers).

The time-series of Barents Sea capelin (*Mallotus villosus*) covers the period from 1945 to 2000. The data series of biomass from 1945 to 1995 is provided by Marshall *et al.* (2000), and that from 1995 to 2000 by ICES (2001a).

## Systems theory

The biomass in the Barents Sea is related to a complex food-chain system. In this investigation the Barents Sea is modelled by the simplified general-system architecture

$$S(t) = \{B_B(t), \{S_n(t), S_o(t), S_f(t), S_{ca}(t), S_{he}(t), S_{co}(t), S_v(t)\}\} \quad (1)$$

where  $S_n(t)$  is the lunar-nodal system,  $S_o(t)$  the ocean system,  $S_f(t)$  the food-chain system,  $S_{ca}(t)$  the capelin-biomass system,  $S_{he}(t)$  the herring-biomass system,  $S_{co}(t)$  the cod-biomass system,  $S_v(t)$  an unknown source, and  $B_B(t)$  is the mutual binding between the Barents Sea system elements. According to Equation (1) the Barents Sea system is expected to be time varying, structurally unstable, and mutually state-dependent. In a mutually related system, a stationary dominant energy source will influence the others.

## The lunar-nodal cycle

The lunar-nodal cycle represents the moving cross-point between the Moon plane-cycle and the ecliptic plane to the Sun. This cross-point describes a lunar-nodal cycle of 18.6134 years. The corresponding cycle of changing inclination of the Moon's orbit to the Earth's equatorial plane is described by the model

$$u_n(t) = 23^\circ 27' + 5^\circ 09' \sin(\omega_0 t + 1.0\pi) \quad (2)$$

where  $\omega_0 = 2\pi/T_0 = 2\pi/18.6134$  (rad/year) is the lunar-nodal angle frequency and  $t$  (year) is the time. The cycle amplitude has a maximum in November 1987 and a minimum in March 1996. The lunar-nodal cycle introduces a 18.6-year gravity-force cycle from the Moon. This cycle produces the 18.6-year lunar-nodal tide in the Atlantic Ocean and the 18.6-year nutation of the Earth axis.

## Biomass state dynamics

The system-state dynamics of stock numbers may be represented by the state differential equation

$$\dot{X}(t) = A(t)X(t) + B(t)U(t) + V(t) \quad (3)$$

where  $X(t)$  represents a  $[n \times 1]$  state vector of the year-class stock numbers,  $A(t)$  a  $[n \times n]$  system-growth matrix,  $U(t)$  a  $[n \times 1]$  vector from a known source of

catch,  $B(t)$  a  $[n \times n]$  binding matrix from the  $U(t)$  vectors,  $V(t)$  a  $[n \times 1]$  disturbance vector from an unknown source  $S_v(t)$ , and  $n$  is the maximum age numbers in the biomass. The disturbance  $V(t)$  is expected to have a non-correlated red spectrum. The system-growth matrix  $A(t)$  has the elements

$$A(t) = \begin{bmatrix} R(t)Ma(t) \\ S(t) \end{bmatrix} \quad (4)$$

where  $R(t)$  is the recruitment-rate function,  $Ma(t)$  a  $[1 \times n]$  maturing vector, and  $S(t)$  is a  $[(n - 1) \times n]$  survival matrix.

### Biomass eigen-frequency

From the state-dynamic model (Equations (3) and (4)), we may formulate the recursive-recruitment model

$$\begin{aligned} x_0(t) &= R(t)Ma(t)x_s(t) + v(t) \\ x_0(t) &= R(t)Ma(t)S_n(t)x_0(t - \tau) + v(t) \\ x_0(t) &= K(t)x_0(t - \tau) + v(t) \end{aligned} \quad (5)$$

where  $x_0(t)$  is the recruited-stock numbers,  $x_s(t)$  a year-class of spawning-stock numbers,  $R(t)$  the recruitment rate,  $Ma(t)$  the spawning rate,  $S_n(t)$  the survival rate from recruitment to the spawning biomass, and  $\tau$  is the delay-time from recruitment to a maximum spawning-year class.

According to the general-system model (Equation (1)) there is a binding from the lunar-nodal system  $S_n(t)$  to the ocean systems  $S_o(t)$  and to the biomass food chain in the Barents Sea. An analysis of the recruitment rate of Northeast Arctic cod and Barents Sea capelin has identified an exponential relationship between the recruitment rate  $R(t)$  and the stationary Kola temperature cycles of 6.2 and 18.6 years (Yndestad, 1996a, b, 1999a, b; Yndestad and Stene, 2002). This relation may be expressed by the simplified model

$$K(t) = K \exp(k_1 U(6, t) + k_2 U(18, t)) \quad (6)$$

where  $K$  is the recruitment number per spawning biomass,  $k_1$  and  $k_2$  the binding to the Kola temperature cycles,  $U(6, t)$  the 6.2-year Kola temperature cycle, and  $U(18, t)$  is the 18.6 year Kola temperature cycle. The time-variant recruitment property (Equations (5) and (6)) introduces a:

1. maximum biomass-growth period when  $U(6, t)$  and  $U(18, t)$  are in a positive state;
2. mean biomass growth when  $U(6, t)$  or  $U(18, t)$  is in a negative state;
3. minimum biomass growth when  $U(6, t)$  and  $U(18, t)$  are in a negative state.

### The code of long-term biomass cycles

Long-term growth is represented by growth in a set of biomass life cycles. We have a:

1. long-term biomass growth when  $U(6, t)$  and  $U(18, t)$  are positive in a set of life cycles;
2. short biomass growth when  $U(6, t)$  or  $U(18, t)$  is negative in a set of life cycles;
3. biomass collapse when  $U(6, t)$  and  $U(18, t)$  are negative in a set of life cycles.

### Frequency modulation

A Fourier transformation of Equation (5) has the frequency transfer-function

$$\frac{x_0(j\omega)}{v(j\omega)} = \frac{1}{1 - Ke^{-j\omega\tau}} \quad (7)$$

when  $K(t) = K$ . This function system is asymptotically stable when  $K < 1$ . Equation (7) has a singularity for when  $K = 1$ ,  $\omega\tau = 2\pi n$ , and  $n = 0, 1, 2, 3, \dots, N$ . A singularity at an angle-frequency cycle  $\omega_e$  means that the recruitment  $x_0(t)$  will have a frequency cycle  $x_0(j\omega_e)$  where the amplitude is amplified to infinity. A singularity in the frequency function will introduce a stochastic resonance in the biomass. In this paper a resonance frequency is called an eigen-frequency. The biomass eigen-frequency cycle is observed at the maximum biomass year class (Yndestad and Stene, 2000). When  $K(t) = K \exp(j\omega_0 t)$  the transfer-function has singularities for  $K = 1$  and  $(\omega\tau + \omega_0 t) = 2\pi n$ . This transfer-function has singularities at  $\tau = 0$ ,  $\omega_3\tau = \omega_0 t$ , and  $\omega\tau = \omega_0 3t$ . Consequently an interaction between the recruitment feedback (Equations (5) and (7)) and the stationary forced cycle (Equation (6)) is expected to introduce a 3. harmonic and a 3. sub-harmonic cycle in the biomass time-series. When  $\omega_0 = 2\pi/T_0 = 2\pi/18.6$  (rad/year), there will be singularities in cycles of  $T_0 = 18.6$ ,  $T_0/3 = 6.2$ , and  $3T_0 = 55.8$  years.

### Cycle identification

The gravity from the stationary 18.6-year lunar-nodal cycle is expected to have an influence on all the elements of the Barents Sea system (Equations (2) and (3)). We may then present the hypothesis that time-series from the Barents Sea have a set of stationary cycles represented by the state model

$$x(t) = \sum_k U(k, t) + v(t) \quad (8)$$

$$U(k, t) = u(k, t) \sin(k\omega_0 t + \varphi(k, t))$$

where  $x(t)$  is the measured time-series,  $U(k, t)$  a dominant stationary cycle,  $k$  a cycle period, and  $v(t)$  is a disturbance from an unknown source. The temporary stationary cycle  $U(k, t)$  has an amplitude  $u(k, t)$ , an angle frequency  $\omega_k = 2\pi/k$ , (rad/year), and a time-variant phase angle  $\varphi(k, t)$ .

The time-series are analyzed by a wavelet transformation to identify a dominant cycle period  $U(k,t)$  and the time-variant phase angle  $\varphi(k,t)$ . The set of dominant cycle periods are identified by a four-step investigation. The first step is to compute the wavelet spectrum by the transformation

$$W(a,b) = \frac{1}{\sqrt{a}} \int_{\mathbb{R}} x(t) \Psi\left(\frac{t-b}{a}\right) dt \tag{9}$$

where  $x(t)$  is the analyzed time-series and  $\Psi()$  is the wavelet-impulse function,  $W(a,b)$  a set of wavelet cycles,  $b$  the translation in time and  $a$  is the time-scaling parameter in the wavelet transformation. The computed wavelets  $W(a,b)$  represent a correlation between  $x(t)$  and the impulse functions  $\Psi()$  over the whole time-series  $x(t)$ . The Coiflet3 wavelet transformation was chosen after many trials on tested data. By this wavelet transformation it is possible to identify single long-period cycles in short time-series. Errors in long-period estimates are reduced by the “sym” property in Matlab (Daubechies, 1992; Matlab, 1997).

The computed wavelet transformation has a set of wavelets  $W(1,\dots,m,b)$ . Dominant wavelet cycles in  $W(1,\dots,m,b)$  have a maximum amplitude as the result of the best correlation to cycles in the time-series  $x(t)$ . The most dominant cycle  $W(k,b)$  in the wavelet set  $W(1,\dots,m,b)$  is identified by a maximum cycle amplitude. The source of a dominant wavelet cycle  $W(k,b)$  is identified by computing the cross-correlation coefficient  $r(k)$  between a dominant wavelet cycle  $W(k,b)$  and a known stationary cycle  $U(k,t)$ . The phase delay between time-series is identified by the phase difference  $\varphi_d(k,t) = \varphi_i(k,t) - \varphi_j(k,t)$ .

## Results

The Barents Sea system (Equation (1)) has a mutual interaction  $B(t)$  between the Earth-nutation system  $S_n(t)$ , the ocean system  $S_o(t)$ , the food-chain system  $S_f(t)$ , and the fish-biomass systems  $S_r(t)$ . According to the general-systems theory a dominant 18.6-year gravity-force cycle from lunar-nodal cycle  $S_n(t)$ , will influence all the others. In this investigation long-term cycles of the Kola Section temperature in the Barents Sea, Norwegian spring herring, Northeast Arctic cod and Barents Sea capelin are analyzed.

### Kola Section temperature

The oceanographic system  $S_o(t)$  is a complex time-variant dynamic process influenced by sea currents and atmospheric conditions. To reduce complexity, the Kola Section data are chosen as a climate indicator to represent the temperature in the Barents Sea.

The Kola Section time-series is an indicator of Atlantic inflow to the Barents Sea. A wavelet transform (Equation (9)) of the Kola temperature series  $x_K(nT)$  has a wavelet set  $W_K(1:80,nT)$ . In this wavelet set the dominant cycles  $W_K(6,nT)$ ,  $W_K(18,nT)$ ,  $W_K(55,nT)$ , and  $W_K(74,nT)$ , are identified and they have a cycle time of 6, 18, 55, and 74 years, respectively (Figure 1). The 6-year wavelet  $W_K(6,nT)$  has a maximum at the years 1907, 1915, 1921, 1930, 1937, 1944, 1951, 1961, 1975, 1983, and 1991, the 18-year wavelet  $W_K(18,nT)$  has a maximum at the years 1909, 1922, 1935, 1955, 1973, and 1991, the 55-year wavelet  $W_K(55,nT)$  has a maximum in 1945 and 2000. The correlation coefficient between the data series  $x_K(nT)$  and

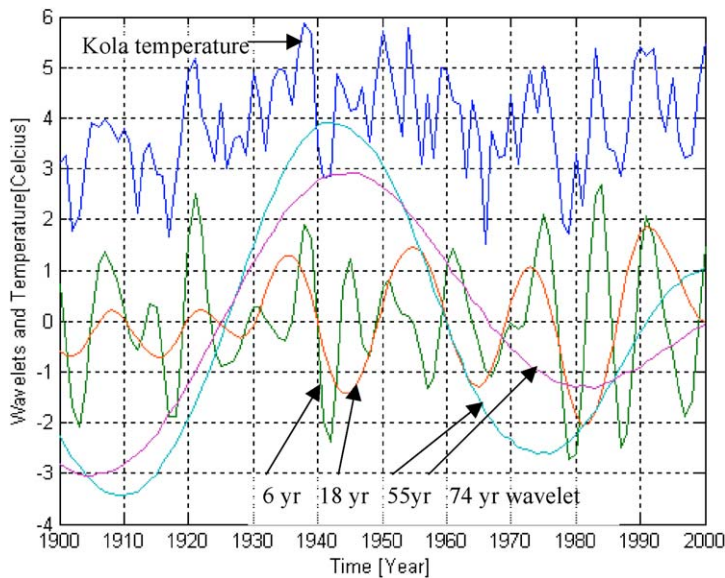


Figure 1. The time-series of Kola Section temperature series and the dominant 6-, 18-, 55-, and 74-year wavelet cycles.

the estimated, dominant wavelet cycles is  $r_{uw} = 0.73$ . The identified, dominant wavelet cycles are correlated to the lunar-nodal cycles

$$\begin{aligned}
 U_K(74, nT) &= u_K(74, nT) \sin(\omega_n nT / 4 + 0.29\pi) \\
 &\text{when } n = 1900, \dots, 2000 \\
 U_K(55, nT) &= u_K(55, nT) \sin(\omega_n nT / 3 + 0.90\pi) \\
 &\text{when } n = 1900, \dots, 2000 \\
 U_K(18, nT) &= u_K(18, nT) \sin(\omega_n nT + \phi_K(18, nT)) \\
 &\text{when } n = 1900, \dots, 2000 \\
 U_K(6, nT) &= u_K(6, nT) \sin(3\omega_n nT + \phi_K(6, nT)) \\
 &\text{when } n = 1900, \dots, 2000
 \end{aligned} \tag{10}$$

The 74-year cycle  $W_K(74, nT)$  has a trend shift in 1925 and 1960, minimum values in 1905 and 1980, and a maximum in 1945. The cross-correlation coefficient between the wavelet cycles  $W_K(74, nT)$  and  $W_K(55, nT)$ , and the lunar-nodal cycles  $U_K(74, nT)$  and  $U_K(55, nT)$ , are  $r_{uw}(74) = 0.95$  and  $r_{uw}(55) = 0.89$ . The 74-year cycle introduces a phase reversal on the 18- and 6-year cycles. The phase angle  $\phi_K(18, nT) = 0.90\pi$  (rad) in the period  $n = 1930, \dots, 2000$  and  $\phi_K(18, nT) = 1.90\pi$  in the period  $n = 1900, \dots, 1930$ . There was a phase reversal when the 74-year cycle shifted from a negative to a positive state. The correlation coefficient  $r_K(18) = 0.90$  when the phase angle  $\phi_K(18, nT)$  is shifted in this period. The 6-year cycle has a correlation coefficient  $r_K(6) = 0.4$  when  $\phi_K(6, nT) = -0.09\pi$  (rad) in the period  $n = 1930, \dots, 1970$  and the 74-year cycle is in a positive state. The phase angle has a phase reversal to  $\phi_K(6, nT) = -1.09\pi$  (rad) in the period  $n = 1970, \dots, 2000$  when the 74-year cycle is in a negative state.

The phase relation between the dominant Kola temperature cycles is expected to have a major influence on the biomass growth in the Barents Sea (Equations (4)–(7)). The identified 6- and 18-year wavelet cycles are positive at the same time in the years 1907, 1921, 1937, 1951, 1975, and 1991. According to the code of long-term growth we may expect a

- Maximum biomass-growth period from 1920, ..., 1937
- Medium biomass-growth period from 1900, ..., 1920 and 1945, ..., 1975
- Minimum recruitment or biomass collapse in 1905, 1942, 1966, and 1979

### Norwegian spring-spawning herring

The Norwegian spring-spawning herring system  $S_h(t)$  may be modelled by the simplified general system  $S(t) = \{B_B(t), \{S_n(t), S_o(t), S_f(t), S_{ca}(t), S_{he}(t), S_{co}(t), S_v(t)\}\}$  (Equation (1)) where  $B_B(t)$  represents a mutual binding between each system element. In this simplified system the

capelin system  $S_{ca}(t)$ , the herring system  $S_{he}(t)$ , and the cod system  $S_{co}(t)$  are mutually related as food and predators. If the nodal system  $S_n(t)$  influences the food chain, it will influence the biomass long-term growth.

The spawning-biomass time-series of Norwegian spring-spawning herring has a mean weight-of-age vector

$$X_{S_{he}}(\text{age}) = \begin{bmatrix} 0 & 0.5 & 14.0 & 94.8 & 37.4 \\ 569.9 & 561.2 & 428.7 & 332.9 & 281.0 \end{bmatrix} 1000 \text{ tons}$$

Maximum spawning biomass is 569 900 tons at the age of 6 years. The herring biomass then has an eigen-frequency of about  $X_{he}(j\omega_e) = 2\pi/T_{he} = 2\pi/6.2$  (rad/year). The herring biomass eigen-frequency cycle of  $T_{he} = 6.2$  years and the interacting dominant Kola temperature cycles of  $T_0/3 = 6.2$ ,  $T_0 = 18.6$  and  $3T_0 = 55.8$  years are expected to introduce dominant, harmonic biomass cycles of  $T_{her} = 6.2$ ,  $3T_{her} = 18.6$ , and  $6T_{her} = 55.8$  years (Equation (7)).

### Herring recruitment rate

The herring recruitment-rate time-series is computed by  $R_{he}(nT) = x_0(nT)/x_S(nT)$  from 1907 to 1999 where  $x_0(nT)$  is the recruited numbers (in millions) of herring and  $x_S(nT)$  is the spawning biomass (tons) (Figure 2). A wavelet transform (Equation (9)) of the recruitment-rate time-series  $R_{he}(nT)$  has the wavelet set  $W_{he}(1:80, nT)$ . In this wavelet set the dominant cycles are  $W_{R_{he}}(6, nT)$ ,  $W_{R_{he}}(18, nT)$ , and  $W_{R_{he}}(55, nT)$ , which have a cycle time of 6, 18, and 55 years (Figure 1). The 6-year wavelet  $W_{R_{he}}(6, nT)$  has a maximum value at the years 1913, 1918, 1924, 1930, 1937, 1944, 1950, 1957, 1963, 1983, and 1993; the 18-year wavelet  $W_{R_{he}}(18, nT)$  has a maximum value at the years 1920, 1938, 1973, and 1992, and the 55-year wavelet  $W_{R_{he}}(55, nT)$  has a maximum value at the years 1927 and 1982. The cross-correlation coefficient between the herring spawning-biomass recruitment rate  $R_{he}(nT)$  and the dominant wavelet cycles  $W_{R_{he}}(nT) = [W_{R_{he}}(6, nT) + W_{R_{he}}(18, nT) + W_{R_{he}}(55, nT)]$  is  $r_{xw} = 0.60$ . The estimated recruitment wavelet cycles  $W_{R_{he}}(6, nT)$  and  $W_{R_{he}}(18, nT)$  have a maximum at about the same years as the Kola temperature cycle  $W_K(6, nT)$  and  $W_K(18, nT)$  in the period  $n = 1910, \dots, 1950$  and from  $n = 1970, \dots, 2000$ . This means that the recruitment cycles of herring have the same cycle time and phase as the Kola Section temperature cycles.

The identified recruitment-rate wavelet cycles confirm the code of long-term growth (Equations (7) and (11)). There was a set of three 6-year cycles in the period from 1920 to 1937 when the 6- and 18-year Kola temperature cycles were positive at the same time. The same situation happened in the period 1972–1991. From 1937 to 1950 there was a period of about  $2 \times 6.2 = 12.4$  years to the next optimum recruitment in 1950. The next optimal recruitment came in 1972. The recruitment came after a period of  $4 \times 6.2 = 24$  years. The estimated 55-year

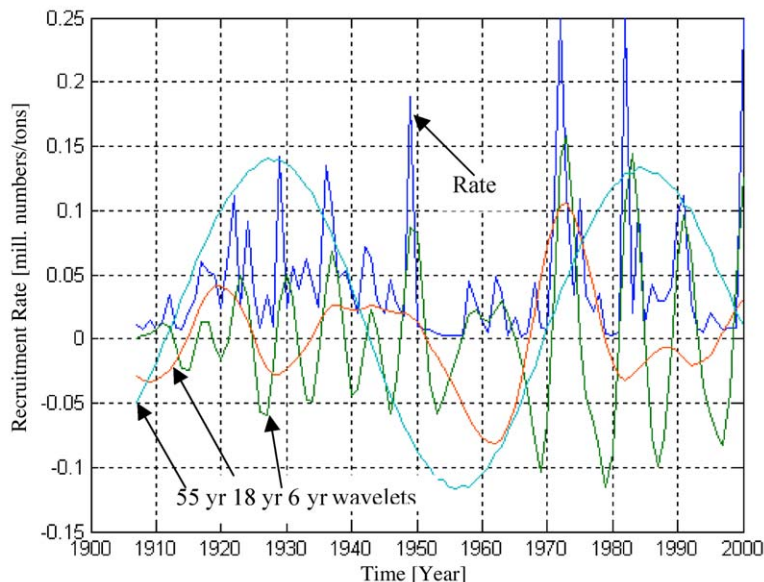


Figure 2. Herring recruitment rate and the dominant wavelet cycles of 6, 18, and 55 years.

cycle  $W_{r_{he}}(55, nT)$  has information about the mean dynamic trend of the recruitment rate. The 55-year wavelet cycle has a maximum in 1937 and 1982.

### Herring stock number

Figure 3 shows the stock-number time-series of Norwegian spring-spawning herring from 1906 to 2000 and the identified dominant wavelet cycles of 6, 18, and 55 years. The 6-year wavelet cycle  $W_{n_h}(6, nT)$  has a maximum value at the years 1919, 1925, 1932, 1938, 1945, 1951, 1959, 1984, 1992, and 2000, the 18-year wavelet  $W_{n_h}(18, nT)$  has a maximum value at the years 1922, 1938, 1964, and 1994, and the 55-year cycle  $W_{n_h}(55, nT)$  has a maximum value in 1935 and 1995. The identified dominant wavelet cycles of stock numbers have a delay of about 1 year compared to the recruitment-rate wavelet cycles. The data series is influenced by a collapse in the period 1965–1990 which was caused by overfishing. The cross-correlation coefficient between the herring spawning-biomass recruitment rate  $R(nT)$  and the dominant wavelet cycles  $W_{n_{he}}(nT) = [W_{n_{he}}(6, nT) + W_{n_{he}}(18, nT) + W_{n_{he}}(55, nT)]$  is  $r_{Rw} = 0.81$ . The wavelet cycles of stock numbers are closely related to the recruitment-rate wavelet cycles since stock numbers are dominated by 1-year recruitment. The estimated wavelet cycles show that the stock numbers have modulated cycles of about  $T_{he} = 6.2$ ,  $3T_{he} = 18.6$ , and  $6T_{he} = 55.8$  years which are harmonic cycles of the biomass eigen-frequency cycle time of  $\tau_{he} = 6.2$  years.

The stock number increased in the growth period from 1920 to 1937 when the 6.2- and 18.6-year Kola cycle were positive at the same time. The stock numbers were reduced to a medium level in the period from 1945 to 1970 when the

6.2- and 18.6-year Kola temperature cycle were not positive at the same time. In 1965 the 6.2- and 18.6-year cycle were negative at the same time and there was a collapse in the stock numbers. The 55-year wavelet cycle  $W_{n_{he}}(55, nT)$  describes the position of the mean number of herring. This cycle has a maximum in 1937 and 1995.

This analysis shows that the stock-number reduction started about 1937 when there was no longer a match between the optimum Kola temperature cycles and the biomass eigen-frequency cycle. When the biomass collapsed in 1965 there was a minimum condition of new recruitment (Equation (11)). The biomass collapse must then be a combination of climate change and overfishing.

### Herring biomass

Figure 4 shows the biomass time-series  $x_{b_{he}}(nT)$  of Norwegian spring-spawning herring from 1906 to 2000 and the identified, dominant biomass-wavelet cycles of 6, 18, and 55 years. The 6-year wavelet cycle  $W_{b_{he}}(6, nT)$  has a maximum in 1910, 1929, 1927, 1924, 1945, 1955, 1964, and 1998, the 18-year wavelet  $W_{b_{he}}(18, nT)$  has a maximum in 1910, 1918, 1952, and 1995, and the 55-year cycle  $W_{b_{he}}(55, nT)$  in 1940 and 2000. In this data series the biomass had a collapse in the period 1965–1990 which was caused by overfishing. The cross-correlation coefficient between the herring spawning-biomass time-series  $x_{b_{he}}(nT)$  and the dominant wavelet cycles sum  $W_{b_{he}}(nT) = [W_{b_{he}}(6, nT) + W_{b_{he}}(18, nT) + W_{b_{he}}(55, nT)]$ , is  $r_{xw} = 0.81$ . The estimated wavelet cycles show the biomass has modulated cycles of about  $T_{he} = 6.2$ ,  $3T_{he} = 18.6$ , and  $6T_{he} = 55.8$  years which are harmonic cycles of the biomass-resonance cycle time of  $\tau_{he} = 6.2$  years.

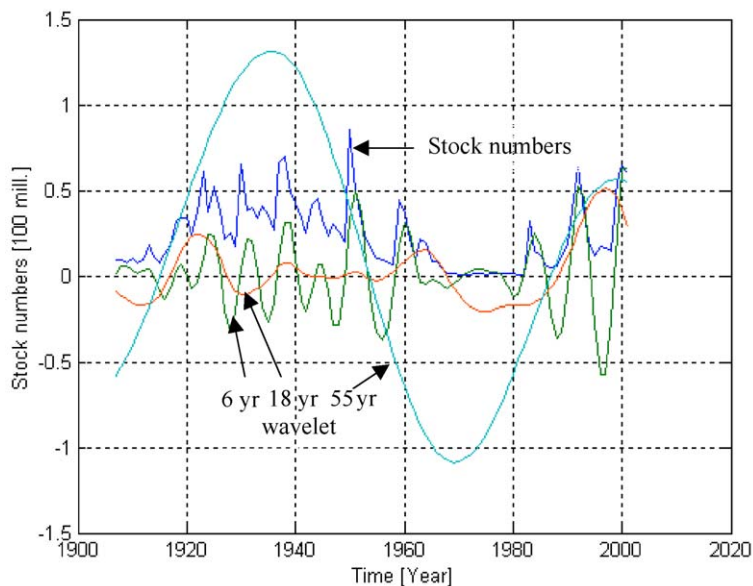


Figure 3. Stock numbers (100 million) of Norwegian spring-spawning herring and the dominant wavelet cycles of 6, 18, and 55 years.

The 6- and 18-year Kola Section temperature cycles were positive at the same time in 1921, 1930, and 1937. In this period there was an optimum recruitment of three life cycles. Each life cycle had a cycle time of about 6 years and the biomass grew over the long-term from about 5–25 million tons (Figure 4). In 1942 the 6- and 18-year Kola cycles were negative at the same time. This introduced a collapse situation and the biomass growth had a turning point. In 1945 only the 6-year Kola cycle temperature was

positive and the biomass was slightly reduced. After a period of  $2 \times 6.2$  years the 6- and 18-year Kola cycles were again positive at the same time. The optimal condition kept the level of the large biomass for about 5 years.

From 1950 there were four optimal life cycles in a period of about  $4 \times 6.2 = 24.8$  years before there was a new optimum Kola temperature-cycle condition in 1975. In this period there was no optimum growth condition over a set of biomass life cycles and the biomass was reduced to about

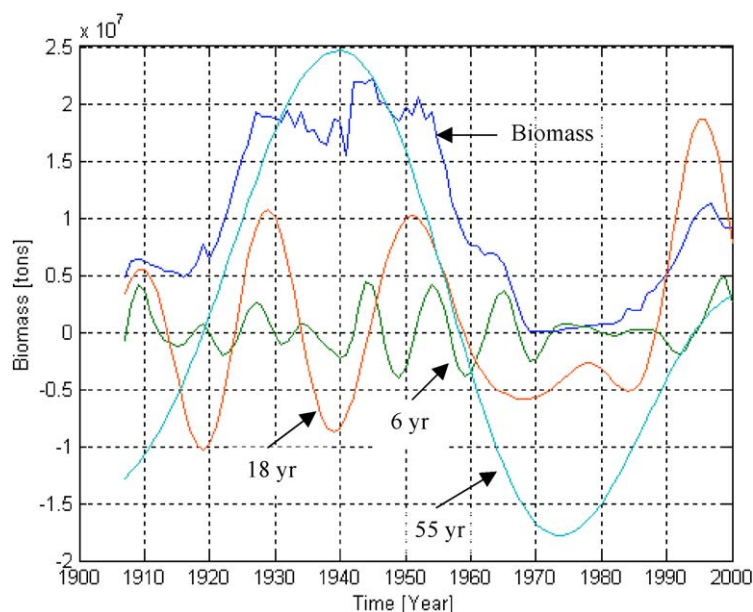


Figure 4. The biomass of Norwegian spring-spawning herring and the 6-, 18-, and 55-year wavelets.

seven million tons in 1960. In 1965 the 6- and 18-year Kola temperature cycles were negative at the same time and there was a total collapse in the biomass. It has been a common belief that the biomass collapse in 1965 was caused by overfishing. This analysis shows that the biomass reduction started about 25 years earlier.

The 6- and 18-year Kola temperature cycles were positive again in 1975 and 1991. A positive 6-year Kola cycle introduced a small growth in 1972 and 1982 (Figures 1–3) and when both temperature cycles were positive in 1991, the biomass again increased to about 10 million tons.

### Northeast Arctic cod

The Northeast Arctic cod system  $S_{co}(t)$  is part of the simplified Barents Sea system  $S(t) = \{B_B(t), \{S_n(t), S_o(t), S_f(t), S_{ca}(t), S_{he}(t), S_{co}(t), S_v(t)\}\}$  (Equation (1)) where  $B_B(t)$  represents binding between each system element. In this simplified system there is a mutual relation between all systems. If there is one stationary energy source, it will influence the cod system.

The spawning-biomass time-series of Northeast Arctic cod has a mean weight-of-age vector

$$X_{s_{co}}(\text{age}) = \begin{bmatrix} 0 & 201 & 6078 & 20341 & 65388 \\ 103012 & 93124 & 63528 & 41586 & 13932 \end{bmatrix} \text{ tons}$$

from age 1 until age 10 years. The maximum biomass year class is 103 012 tons at the age of 6 years. Then the cod biomass has an eigen-frequency at about  $X_{co}(j\omega_c) = 2\pi/T_{co} = 2\pi/6.2$  (rad/year). This means that the biomass of Northeast Arctic cod has a resonance close to the  $\tau_{co} = 6.2$  years which is the same cycle time as the biomass eigen-frequency cycle time  $\tau_{he}$  of Norwegian spring-spawning herring and the Kola temperature cycle of  $T_K/3 = 6.2$  years. The cod-biomass cycle time  $\tau_{he} = 6.2$  years and the interacting dominant Kola temperature cycles of  $T_K/3 = 6.2$ ,  $T_K = 18.6$  and  $3T_K = 55.8$  years are expected by the approach taken here to introduce dominant cycles of  $T_{co} = 6.2$ ,  $3T_{co} = 18.6$ , and  $6T_{co} = 55.8$  years (Equation (7)).

### Cod biomass

A wavelet transform (Equation (9)) of the time-series  $x_{co}(nT)$  of Northeast Arctic cod has identified a set of wavelets  $Wb_{co}(1:50, nT)$  (Figure 5). The computed wavelet set has dominant wavelets of 6 and 18 years. The 6-year wavelet  $Wb_{co}(6, nT)$  has a maximum value at about the years 1903, 1912, 1923, 1926, 1936, 1945, 1955, 1961, 1968, 1975, 1986, and 1993, and the 18-year wavelet  $Wb_{co}(18, nT)$  has a maximum value at the years 1906, 1925, 1941, 1952, 1973, and 1995. The cross-correlation coefficient between the biomass time-series  $x_{co}(nT)$  and the identified dominant wavelet cycles sum  $Wb_{co}(nT) =$

$[Wb_{co}(6, nT) + Wb_{co}(18, nT) + Wb_{co}(55, nT)]$  is  $r_{xw} = 0.87$ . The dominant wavelet cycles have the same cycle time as the dominant Kola Section temperature cycles, but lag by about  $\tau_{co} = 6.2$  years. This delay is the time from recruitment to a maximum year class of about 6 years. The estimated 55-year wavelet is influenced by low fishing activity from 1940 to 1945 and in 1983 there was a collapse in the biomass.

The identified dominant biomass cycles confirm the code theory of long-term growth (Equations (7) and (11)). The biomass of Northeast Arctic cod had a growth period from 1920 to 1945 when the 6- and 18-year Kola Section cycles were positive at the same time in 1921, 1930, and 1937. After a delay of about 6 years ( $\tau_{co}$  years) the cod biomass was maximum in 1928, 1940, and 1946. The biomass had a reduction from 1945 to 1980. Again the 6- and 18-year Kola cycles were positive at the same time only in the years 1962, 1973, and 1975. In these years the biomass had a small growth in 1960 and a strong growth in 1968 and 1975. These estimates demonstrate that the biomass of Northeast Arctic cod grows when the 6-, 18-, and 55-year Kola Section temperature cycles are positive. This analysis shows that the long-term biomass cycles of Northeast Arctic cod have the same character as the long-term cycles of Norwegian spring-spawning herring.

### Cod catch

It is a common belief that there is a close relationship between catch and stock numbers and so the same dominant cycles in each parameter are expected (Figure 6). The wavelet set  $Wc_{co}(1:80, nT)$  has been computed from the time-series  $xc_{co}(nT)$  of cod in Lofoten (Godø, 2000) in the period 1864–1978 and does have the same dominant wavelets of 6, 18 and 55 years as estimated in the biomass time-series. The 6-year wavelet cycle  $Wc_{co}(6, nT)$  has a maximum value in the years 1880, 1886, 1896, 1905, 1915, 1921, 1927, 1939, 1946, 1952, 1961, and 1972, the 18-year wavelet cycle  $Wc_{co}(18, nT)$  has a maximum value at the years 1880, 1892, 1910, 1928, 1946, and 1970, and the 55-year wavelet  $Wc_{co}(55, nT)$  has maximum values in the years 1885 and 1938. The cross-correlation coefficient between the time-series of catch and the estimated dominant wavelet cycles  $Wc_{co}(nT) = [Wc_{co}(6, nT) + Wc_{co}(18, nT) + Wc_{co}(55, nT)]$  is  $r_{xw} = 0.82$ . The dominant wavelet cycles of catch numbers have the same cycle time as in the biomass time-series. The different cycle-phase is explained by the difference between the stock-number distribution and the biomass distribution.

The dominant 6- and 18-year wavelets of the Lofoten catch have the same pattern as the dominant biomass-wavelet cycles. The growth period was from 1920 to 1940, while the decline was from 1940 to 1960. In these data the long-term reduction of biomasses occurs earlier because of less fishing effort in the period 1940–1945. The catch grew from 1877 to 1895 when the 6- and 18-year cycles were positive at the

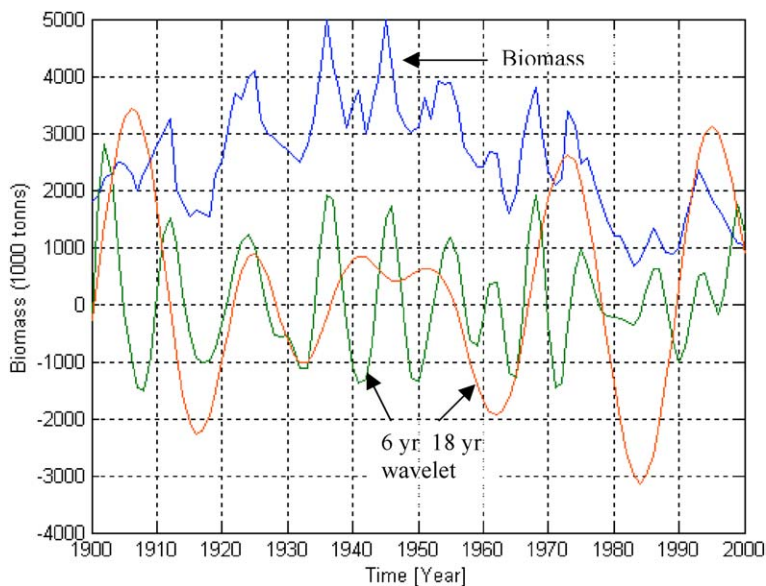


Figure 5. The time-series of the Northeast Arctic cod biomass and computed wavelets of 6 and 18 years.

same time and was reduced in the period 1900–1920 when only in 1908 were the wavelet cycles positive at the same time. The 55-year wavelet indicates that the biomass has a natural long-term fluctuation of about 55 years.

### Barents Sea capelin

The Barents Sea capelin stock is of vital importance in the Arctic food web. It is the main plankton feeder in the area and serves as an important forage fish for other fish stocks,

seals, whales, and sea birds. The capelin is therefore influenced by its abiotic environment and by the abundance of food, predators, and fisheries.

The Barents Sea capelin-system biomass  $S_c(t)$  is thus influenced by a set of external systems in the Barents Sea. The recruitment dynamics of Barents Sea capelin are dependent on a complex set of conditions such as the life-cycle time, the eigen-frequency, the predator life cycles, catch-to-landings, the sea temperature, and food supply. If

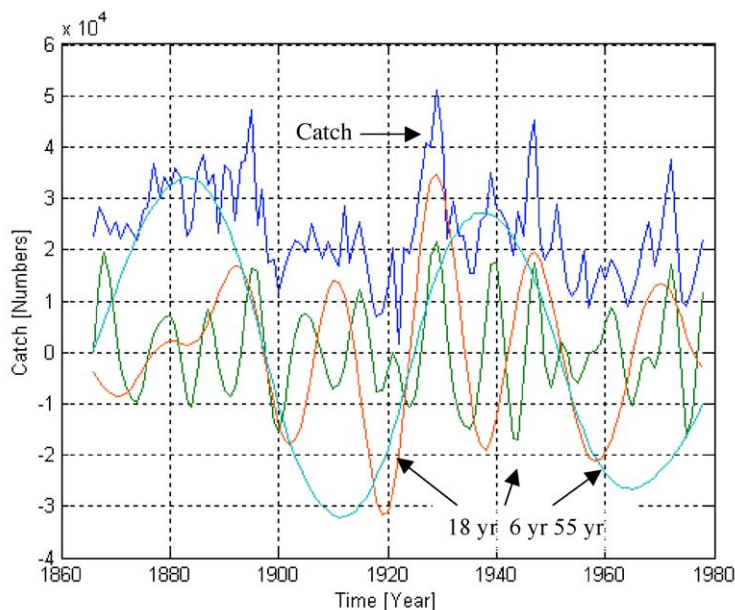


Figure 6. The catch numbers of Northeast Arctic cod at Lofoten and the computed wavelets of 6, 18, and 55 years.

one of these external systems has a dominant property it will influence the long-term capelin dynamics.

The spawning-biomass time-series of Barents Sea capelin has a mean weight-at-age vector  $X_{s_{ca}}(\text{age}) = [0.0 \ 0.0 \ 29.3 \ 12.8 \ 0.3]$  in 1000 tons. Maximum spawning biomass is 29 300 tons at the age of 3 years. This means that the 3-year-old capelin is the most dominant year class in the spawning stock. A frequency analysis of the capelin stock numbers has identified an eigen-frequency cycle time  $\tau_{ca} = 3.1$  years, which introduces large fluctuations in the biomass (Yndestad and Stene, 2001).

The interacting Kola Section temperature in the Barents Sea has dominant stationary cycles of  $T_0 = 18.6$  years and  $T_0/3 = 6.2$  years. The eigen-frequency cycle at  $\tau_{ca} = 3.1$  years and the interacting dominant Kola temperature cycles should introduce dominant cycles of  $T_{ca} = 3.1$ ,  $2T_{ca} = 6.2$ ,  $3T_{ca} = 9.3$ , and  $6T_{ca} = 18.6$  years (Equation (7)). A biomass eigen-frequency period of about  $6.2/2 = 3.1$  years implies that the biomass will have a different dynamic property compared to the herring biomass and the cod biomass.

A wavelet transform of the Barents Sea capelin time-series  $x_{ca}(nT)$  from 1946 to 2000 has a set of wavelets  $W_{b_{ca}}(1:30, nT)$ . In this wavelet set there are dominant wavelet cycles of 6 and 18 years. The 6-year wavelet cycle  $W_{ca}(6, nT)$  has a maximum value around the years 1951, 1960, 1969, 1975, 1983, and 1991 and the 18-year wavelet cycle  $W_{ca}(18, nT)$  has a maximum value at about the years 1951, 1975, and 1994. The cross-correlation coefficient between the biomass time-series  $x_{ca}(nT)$  and the dominant wavelet sum  $W_{ca}(nT) = [W_{ca}(6, nT) + W_{ca}(18, nT)]$  is  $r_{xw} = 0.72$ .

The 18-year cycle  $W_{ca}(18, nT)$  has a maximum around the years 1952, 1975, and 1994. This is a growth delay of about  $\tau_{ca} = 3.1$  years compared to the 18-year cycle of the recruitment rate and the 18-year Kola Section wavelet cycle  $W_K(18, nT)$ . Potential errors in these cycle estimates are the short-time series and the collapses of the biomass in 1985 and 1995. The computed wavelet cycles show an 18-year cycle and a higher-frequency cycle shifting between a period of about 6 and 9 years. The 18-year cycle follows the 18-year Kola temperature cycle, which had maximum values at about the years 1955, 1972, and 1991. When the 18-year cycle is in a negative state the biomass growth is dependent on the relationship between the 6-year Kola temperature cycle and the  $6.2/2 = 3.1$  year biomass eigen-frequency cycle. Figure 7 shows that this introduces a 9-year cycle time when the 18-year Kola cycle is negative and a 6-year cycle time when the 18-year Kola cycle is positive. These estimated wavelet cycles confirm that the biomass has modulated cycles of about  $2T_{ca} = 6.2$ ,  $3T_{ca} = 9.3$ , and  $6T_{ca} = 18.6$  years which are sub-harmonic cycles of the biomass eigen-frequency cycle time of  $\tau_{ca} = 3.1$  years.

The recruitment rate  $R(nT)$  has a maximum around the years 1976, 1981–1982, 1989–1990, and 1995–1997

which are close to the maximum of the Kola temperature cycles. The recruitment rate  $R(nT)$  had a maximum when the 6.2-year cycle or the 18.6-year temperature cycle had a maximum (Yndestad and Stene, 2001). This change in the recruitment cycle introduces dominant biomass cycles of about  $2T_{ca} = 6.2$  years when the 18.6-year temperature cycle had a positive state and a cycle of  $3T_{ca} = 9.3$  years when the 18.6-year cycle was in a negative state.

The Barents Sea capelin has a short eigen-frequency cycle time of about  $\tau_{ca} = 3.1$  years. The biomass then has maximum growth each time the 6.2-year Kola cycle is positive. The capelin biomass has a growth time of about three years and a cycle time of about six years. The short eigen-frequency cycle time influences how the biomass-cycle phase is able to adjust to the 6.2- and 18.6-year Kola temperature cycle. The biomass had a maximum growth in period 1951, 1960, 1970, 1975, and 1991 when the 6.2- and 18.6-year Kola temperature cycles were positive at the same time. The biomass had a minimum level in 1950, 1965, 1978, and 1995 when the 6.2-year Kola cycle had a minimum. In 1987 and 1995 the biomass changed from a minimum to a collapse.

When the 6.2- and 18.6-year temperature cycles have a negative state, it takes about  $3\tau_{ca} = 9.3$  years for the adjustment to an optimum condition. In this period the recruitment system (Equation (5)) is shifted from a positive-feedback system to that of negative-feedback. The result is a collapse in the biomass as happened in 1955, 1963, and 1986. The collapse in 1995 was most likely caused by overfishing in the 1980s (Yndestad and Stene, 2001). The short eigen-frequency cycle time of  $\tau_{ca} = 3.1$  years made it possible to adapt the next biomass cycle to the next 6.2-year temperature cycle in 1960 and 1991.

This analysis shows that the biomass of Barents Sea capelin has a long-term growth when the 6- and 18-year Kola Section temperature cycle has a positive state and a pronounced decline when both temperature cycles have a negative state. When the 18-year Kola cycle turns to a negative state the biomass loses the synchronic phase relation between the biomass eigen-frequency cycle and the Kola temperature cycles. After a cycle time of  $3\tau_{ca}$  years there is a new adaptation and a new growth period. In a long time-series this adaptation is shown as a cycle phase reversal and the cycle time is increased from six to nine years.

## Discussion

The dominant biomass dynamics in the Barents Sea are a result of different environmentally random, mutual interactions between the ocean system, the food chain, catch, and a multi-species system (Equation (1)). A frequency analysis of the long-term time-series from this system is expected to be represented by a non-deterministic and non-correlated red spectrum. The approach taken in this paper produces a different result.

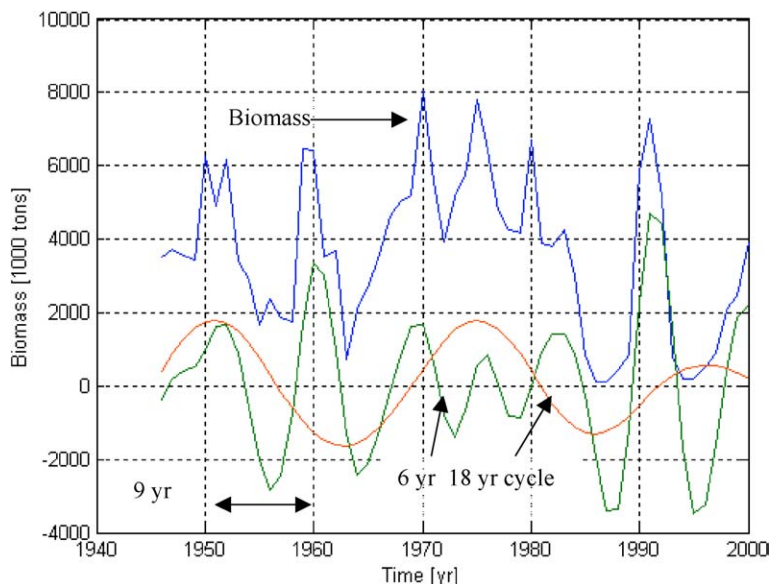


Figure 7. The Barents Sea capelin biomass and the dominant-wavelet cycles of 6 and 18 years.

### The code of biomass dynamics

In this investigation, fluctuations in Kola Section temperatures and the stocks of the Barents Sea capelin, the Norwegian spring-spawning herring and Northeast Arctic cod are analyzed by a wavelet transformation to identify the source of dominant biomass fluctuations. The results show a common source of long-term biomass cycles.

#### *The forced oscillator*

The Kola Section temperature has dominant temperature cycles of about 6.2, 18.6, and 55 years which are related to the 18.6-year lunar-nodal tide. The 18.6-year temperature cycle is expected to be a deterministic cycle controlled by gravity from the Moon. This cycle behaves like a forced, oscillating temperature cycle, which will influence the biomass dynamics in the food chain.

#### *Eigen-frequency biomass cycle*

The biomass of herring, cod and capelin has an eigen-frequency biomass cycle which is adapted to the 6.2-year temperature cycle in the Barents Sea.

#### *The long-term biomass growth*

The long-term biomass growth is related to a set of optimal recruitment periods when the 6- and 18-year Kola Section temperature cycles are positive at the same time. In this period the 6-year eigen-frequency of recruitment has an optimal growth in a period of three to four life cycles.

#### *Long-term biomass reduction*

The long-term biomass reduction is related to a period when the 6- and 18-year Kola Section temperature cycles are not positive at the same time. The growth and reduction

of biomass is therefore not related to the absolute temperature value, but rather to the phase relation between the dominant eigen-frequency cycle and the Kola temperature cycles in the Barents Sea.

#### *The biomass collapse*

The biomass collapse is related to a period when the 6- and 18-year Kola Section temperature cycles are negative at the same time. In this period there are poor conditions of recruitment and growth over a period of two to four life cycles.

#### *The three causes of fluctuation*

There are three causes of fluctuation in the biomasses. The 6-year cycle in herring and cod is caused by the biomass eigen-frequency, which is a feedback property where optimal recruitment is adapted to the 6.2-year Kola temperature cycle. The 18-year biomass cycle is related to a period of about nine years when there was good recruitment. The long-term 55-year cycle is caused by a chain of optimal life cycle recruitment.

The biomass fluctuations in the Barents Sea may be explained by a deterministic model. According to this model the optimum biomass life-cycle time is linked with the Kola temperature cycles of 18.6 and  $18.6/3 = 6.2$  years. Biomass growth, reduction, and collapse are associated with the phase relation between these cycles.

#### The Norwegian spring-spawning herring

The Norwegian spring-spawning herring stock has been characterized by large fluctuations. Norwegian historical records document good herring periods from 1500 to 1570, 1600 to 1650, 1690 to 1774 and from 1808 to 1874 (Vollan,

1971). These records show biomass fluctuations of about 50–80 years. The findings in this paper support the theory that long-term biomass fluctuations in the Barents Sea have a cycle of 55–74 years. The changes from 50 to 80 years may be explained by a time-variant phase in the biomass cycle, which is controlled by the 74-year temperature cycle.

There is a common belief that the collapse in 1965 was caused by overfishing. The results here show that the biomass reduction started 30 years earlier as a climate-driven process. In the long-term period of less recruitment from 1940 to 1965, overfishing increased the speed of biomass reduction. The biomass collapsed in 1965 when the 6- and 18-year temperature cycles were negative at the same time. The new biomass-growth period came from 1992 when the 6.2-, 18.6-, and 55.8-year Kola Section temperature cycles were again in a positive state.

### The Northeast Arctic cod

The wavelet-cycle analysis shows that the Northeast Arctic cod has the same growth and reduction cycles as the Norwegian spring-spawning herring. The dominant cycles of 6.2-, 18.6-, and 55.8-years support cycles of 18.6 years in the biomass identified in earlier studies (Wyatt *et al.*, 1994; Yndestad, 1999b). The adopted 6.2-year biomass eigen-frequency cycle and the 55-year cycle in Lofoten catch, indicates very long-term cycles.

The estimated relationship between biomass cycles and temperature cycles supports the “matching” theory of Hjort (1914) at a macro level. In that paper he analyzed the length distribution of Northeast Arctic cod and explained fluctuations in the biomass as caused by a match between the spawning time and food for the larvae.

### The Barents Sea capelin

The Barents Sea capelin stock has an eigen-frequency cycle of about  $6.2/2 = 3.1$  years. In the time-series from 1945 to 2000 the biomass has an increased growth rate when the 6.2- and 18.6-year Kola Section temperature cycles are in a positive state. The biomass was reduced from six to two million tons in 1955 and in 1964 when the 6.2- or 18.6-year Kola Section temperature cycles were in a negative state. In 1987 there was a new collapse in the biomass. This collapse was partly caused by the lower temperatures when the 6.2- and 18.6-year cycles were in a negative state, and partly by overfishing. The biomass collapse in 1993 is explained by the overfishing in the 1980s, which caused a limited age distribution in the capelin stock (Yndestad and Stene, 2001).

### Some aspects of the materials and methods

The analytical approach that has been taken has some potential sources of errors. For example, there may be errors in the data samples, which cannot be controlled. In this investigation long trends in the data are analyzed and so changes in the methods of estimating data may then

influence the long-term cycles. A potential source of a long-term error in long-term fluctuations is between linked-up time-series. The herring time-series has a link-point in 1946, the cod time-series in 1946, the Lofoten catch in 1958, and capelin from 1995. This may have influenced the phase of the estimated dominant cycles. However, the computed wavelets represent a low-pass filtered data series so that single random data errors are unlikely to be a major problem in their analysis.

The time-series are analyzed by a wavelet transformation to identify the dominant cycle periods and phase relations. The Coiflet3 wavelet transformation (Matlab Toolbox, 1997) was chosen after many trials on tested data. The cycle identification has two fundamental problems. One problem is that of identifying periodic cycles when the phase has a reversal in the time-series. The phase-reversal property of the stationary cycles excludes traditional spectral analysis methods. The problem is solved by first identifying the dominant cycles and correlating the cycles to known reference cycles. A second problem is that of identifying the long-period cycles of 55 and 74 years. This problem is solved by the same method. First, identify the dominant long-wavelet periods and then correlate the periods to a known cycle reference.

The results show a good correlation between the time-series and the dominant wavelet cycles, and there is another good correlation between the dominant wavelet cycles and the lunar-nodal cycles of  $18.6/3 = 6.2$ , 18.6, and  $3 \times 18.6 = 55.8$  years. The close relationship between the lunar-nodal tide cycles and the biomass eigen-frequency is a strong indication of a long-term adopted property. The Kola Section temperature data have dominant stationary cycles that are of the greatest importance in forecasting future biomass cycles in this area.

The 18.6-year Kola Section temperature cycle has a stationary frequency but not always a stationary phase. The phase reversal of the lunar-nodal cycles explains why this cycle has been difficult for others to identify (Ottersen *et al.*, 2000). A closer analysis of the Kola Section temperature series and ice extent in the Barents Sea, has shown that the phase of the 18.6-year temperature cycle has shifted  $180^\circ$  in the period from about 1890 until 1925 when a 74-year cycle was in a negative state (unpublished). In this analysis a 55- and a 74-year temperature cycle in the Barents Sea has been found. The relationship between the two cycles is still unclear. The wavelet analysis of the Kola temperature series indicates that the 55-year temperature cycle is the sum of the 6.2- and 18.6-year cycles where the phase relation between them is slowly changing in a period of  $3 \times 18.6 = 55.8$  years. The 55.8-year cycle may be explained as the envelope of the two cycles. An analysis of the Arctic ice extent indicates that the 74-year cycle has its source in the Arctic Ocean. The fact that the 74-year Kola cycle has the energy to control the phase of the 18-year Kola cycle, explains why the herring biomass has a fluctuation between 50 and 80 years.

## Implications of the results

This analysis shows that the long-term growth of the stocks of herring, cod, and capelin are influenced by a matching between the biomass eigen-frequency and the stationary temperature cycles of 6.2 and 18.6 years in the Barents Sea. The close relationship to the 18.6-year lunar-nodal cycle indicates that the stationary cycles are stationary lunar-nodal tides controlled by gravity from the Moon. These results suggest that we are able to explain the cause of the long-term biomass dynamics in the Barents Sea. The deterministic property of the 18.6-year lunar-nodal tide provides a new way of long-term forecasting over period of 50–80 years or more.

## Acknowledgements

I would like to thank Vladimir Ozhigin at PINRO institute in Murmansk for access to the Kola Section temperature data series, Reidar Toresen at the Institute of Marine Research in Bergen for access to the data series of Norwegian spring-spawning herring and Olav Rune Godø at the Institute of Marine Research in Bergen for access to the data series on the Northeast Arctic cod.

## References

- Bochkov, Y. A. 1982. Water temperature in the 0–200 m layer in the Kola-meridian in the Barents Sea, 1900–1981. Sb. Nauchn. Trud. PINRO, Murmansk, 46: 113–122 (in Russian).
- Daubechies, I. 1992. Ten lectures of wavelet. SIAM Journal on Mathematical Analysis, 24(2): 499–519.
- Gjoseter, H. 1997. Studies of the Barents Sea capelin, with emphasis on growth. Dr scient thesis, Department of Fisheries and Marine Biology, University of Bergen, Norway. Paper III, IV and V.
- Godø, O. R. 2000. Fluctuation in stock properties of arcto-norwegian cod related to long-term environmental changes. IIASA. Interim report IR-00-023. 6 April 2000. Austria. <http://www.iiasa.ac.at/cgi-bin/pubsrch/IR00023>.
- Hamre, J. 2000. Capelin and herring as key species for the yield of Northeast Arctic cod. Results from multispecies model runs. SAP Symposium 4–6 December 2000. Bergen, Norway.
- Helland-Hansen, B., and Nansen, F. 1909. The Norwegian Sea. Report on Norwegian fishery and marine-investigations, Volume II (2), Kristiania.
- Hjort, J. 1914. Fluctuations in the great fisheries of Northern Europe. Conseil Permanent International pour L'Exploration de la Mer, Rapports, II(2):20.
- Hyllen, A. 2002. Fluctuations in abundance of Northeast Arctic cod during the 20th century. ICES Marine Science Symposia, 534–550.
- ICES 2001a. Northern pelagic and blue whiting fisheries working group. ICES CM 2001/ACFM: 17. 18–27 April 2001. Reykjavik.
- ICES 2001b. Report of the Arctic fisheries working group. ICES CM 2001/ACFM: 19. 24 April–3 May 2001. Bergen, Norway.
- Izhevskii, G. K. 1961. Oceanological Principles as Related to the Fishery Productivity of the Seas, 95 pp. Pishcepromizdat, Moscow (Translated 1966: Israel Program for Science Transactions. Jerusalem).
- Izhevskii, G. K. 1964. Forecasting of oceanological conditions and the reproduction of commercial fish. All-Union Science Research Institute of Marine Fisheries and Oceanography. Israel Program for Science Transactions. 22 pp.
- Loder, J. W., and Garret, C. 1978. The 18.6-year cycle of the sea surface temperature in the shallow seas due to tidal mixing. Journal of Geophysical Research, 83: 1967–1970.
- Maksimov, I. V., and Smirnov, N. P. 1964. Long-range forecasting of secular changes of the general ice formation of the Barents Sea by the harmonic component method. Murmansk Polar Science Research Institute, Sea Fisheries, 4: 75–87.
- Maksimov, I. V., and Smirnov, N. P. 1965. A contribution to the study of causes of long-period variations in the activity of the Gulf Stream. Oceanology, 5: 15–24.
- Maksimov, I. V., and Smirnov, N. P. 1967. A long-term circumpolar tide and its significance for the circulation of ocean and atmosphere. Oceanology, 7: 173–178 (English edition).
- Maksimov, I. V., and Sleptsov-Shevlevich, B. A. 1970. Long-term changes in the tide-generation force of the moon and the iciness of the Arctic Seas. Proceedings of the N. M. Knipovich Polar Scientific-Research and Planning Institute of Marine Fisheries and Oceanography (PINRO), 27: 22–40.
- Marshall, T. C., Yaragina, N. A., Ådlandsvik, B., and Dolgov, A. V. 2000. Reconstruction of the stock-recruit relationship for Northeast Arctic cod using a bioenergetic index of reproductive potential. Canadian Journal of Fisheries and Aquatic Sciences, 57: 2433–2442.
- Matlab Toolbox 1997. Users Guide. The Math Works Inc., Natick.
- Nakken, O. 1994. Causes of trends and fluctuations in the Arcto-Norwegian cod stock. ICES Marine Science Symposium, 212–228.
- Ottersen, G., Ådlandsvik, B., and Loeng, H. 2000. Predicting the temperature of the Barents Sea. Fisheries Oceanography, 9(2): 121–135.
- Ottestad, P. 1942. On periodical variations on the yield on the Great Sea Fisheries and the possibility of establishing yield prognoses. Fiskeridirektoratets Skrifter, VII(5).
- Pettersson, O. 1905. On the probable occurrence in the Atlantic Current of variations periodical, and otherwise, and their bearing on metrological and biological phenomena. Rapp. P.-v. R'eun. Cons. perm. int. l'Explor. Mer, 42: 221–240.
- Pettersson, O. 1914. Climatic variations in historic and prehistoric time: Svenska Hydrogr. Biol. Kommissiones Skrifter, No. 5. 26 pp.
- Pettersson, O. 1915. Long-periodical variations of the tide-generating force: Conseil Permanente International pour l'Exploration de la Mer (Copenhagen), Pub. Circ. No. 65, pp. 2–23.
- Pettersson, O. 1930. The tidal force. A study in geophysics. Geografiska Annaler, 18: 261–322.
- Royer, T. C. 1993. High-latitude oceanic variability associated with the 18.6-yr nodal tide. Journal of Geophysical Research, 98(C3): 4639–4644.
- Toresen, R., and Østvedt, O. J. 2000. Variation in abundance of Norwegian spring herring (*Clupea harengus*, Clupeidae) through the 20th century and the influence on climatic fluctuation. Fish and Fisheries, 2000(1): 231–256.
- Vollan, O. 1971. Sildefisken gjennom tusen år. Det Norske Samlaget, Oslo.
- Wyatt, T., Currie, R. G., and Saborido-Ray, F. 1994. Deterministic signals in Norwegian cod records. ICES Marine Science Symposium, 198: 49–55.
- Yndestad, H. 1996a. Stationary temperature cycles in the Barents Sea. The cause of causes. The 84th International ICES Annual Science Conference. Hydrography Committee. 27 September–4 October 1996. Reykjavik, Iceland.
- Yndestad, H. 1996b. Systems dynamics of North Arctic cod. The 84th International ICES Annual Science Conference. Hydrography Committee. 27 September–4 October 1996. Reykjavik, Iceland.

- Yndestad, H. 1999a. Earth nutation influence on the temperature regime in the Barents Sea. *ICES Journal of Marine Science*, 56: 381–387.
- Yndestad, H. 1999b. Earth nutation influence on system dynamics of Northeast Arctic cod. *ICES Journal of Marine Science*, 56: 562–657.
- Yndestad, H. 2002. The code of Norwegian spring spawning herring long-term cycles. *ICES Annual Science Conference*. October 2002. Copenhagen.
- Yndestad, H., and Stene, A. 2001. System dynamics of Barents Sea capelin. *ICES Annual Science Conference*. 26–29 September 2001, Oslo.